Probing Na^+ Induced Changes in the HIV-1 TAR Conformational Dynamics using NMR Residual Dipolar Couplings: New Insights into the Role of Counterions and Electrostatic Interactions in Adaptive Recognition

*Anette Casiano-Negroni, Xiaoyan Sun, and Hashim M. Al-Hashimi**

SUPPORTING INFORMATION

Figure S1. Comparison of HSQC spectra for TAR in the presence and absence of phage in (A) 160 mM Na^+, (B) 320 mM Na^+ and (C) 25 mM Na^+ / 4 mM Mg^{2+}.

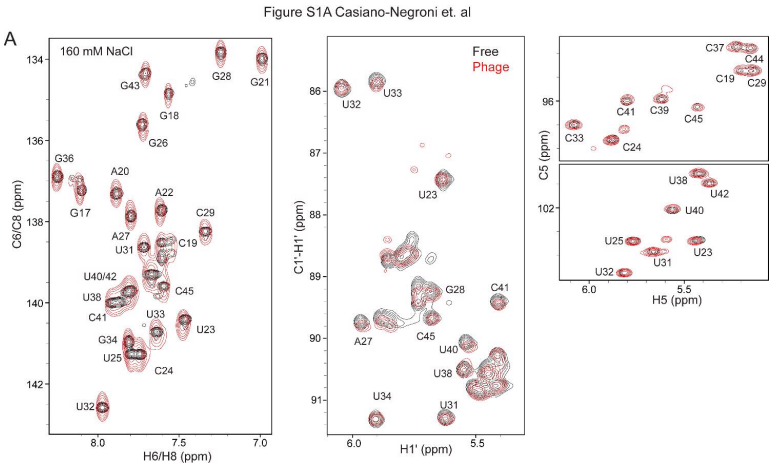

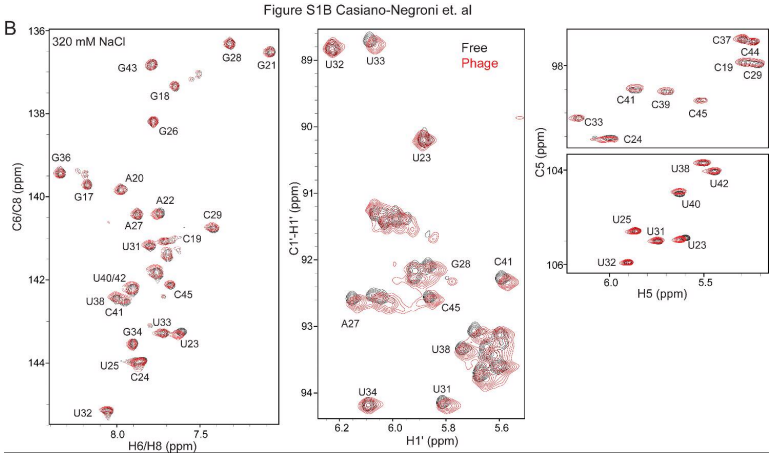

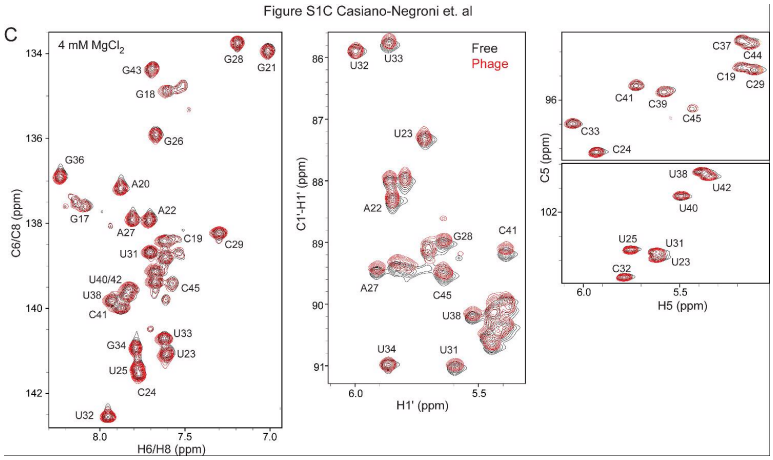

Figure S2. Correlation plot for one bond C-H RDCs measured in 25 mM Na^+ / 4 mM Mg^{2+} TAR using experiments that yield splittings along the ^1H and ^{13}C and dimension.

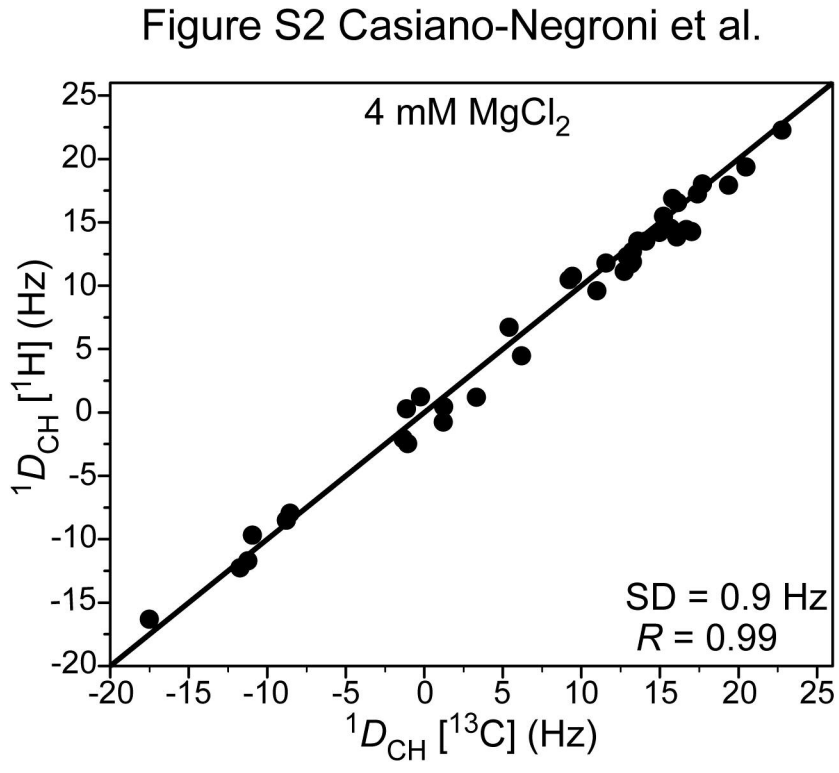

Figure S3. Comparison of one bond C-H RDCs (normalized for differences in degree of order, see legend of Figure 3) measured under different metal conditions.

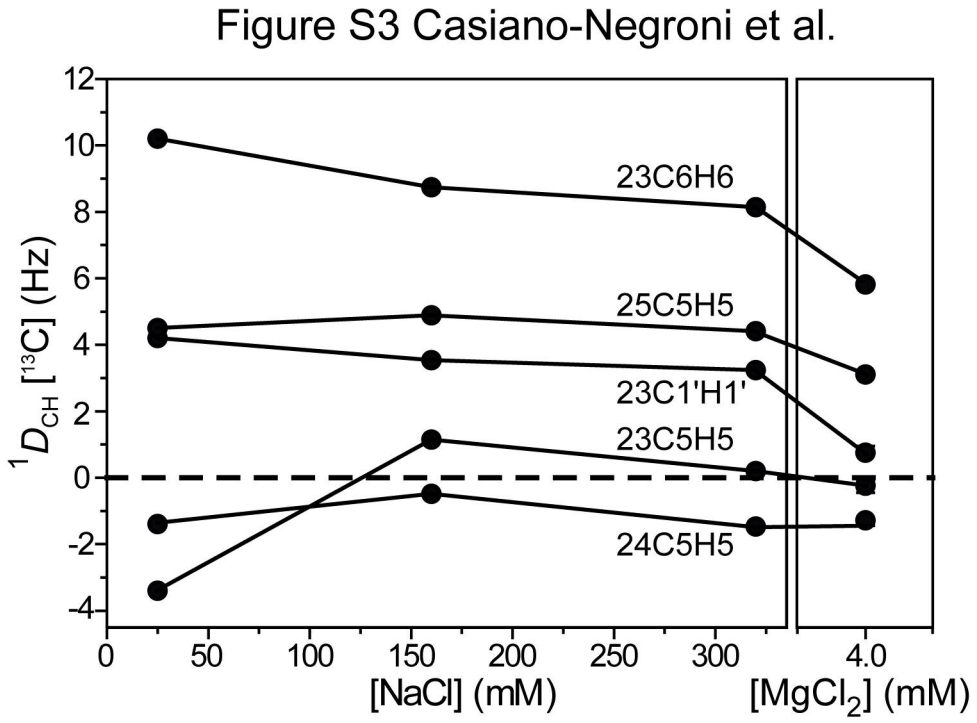

Figure S4. Electrostatic surfaces for the unbound and bound TAR structures (following removal of ligands) for all models of the NMR ensemble. Highlighted in letters are the positions of cationic groups on small molecules relative to the TAR electrostatic surface. The TAR orientation in each case was chosen to illustrate proximity of cationic groups near the strong negative charge potential in TAR. Only one NMR model was provided for structures Rbt 158, Rbt 203, and Rbt 550.

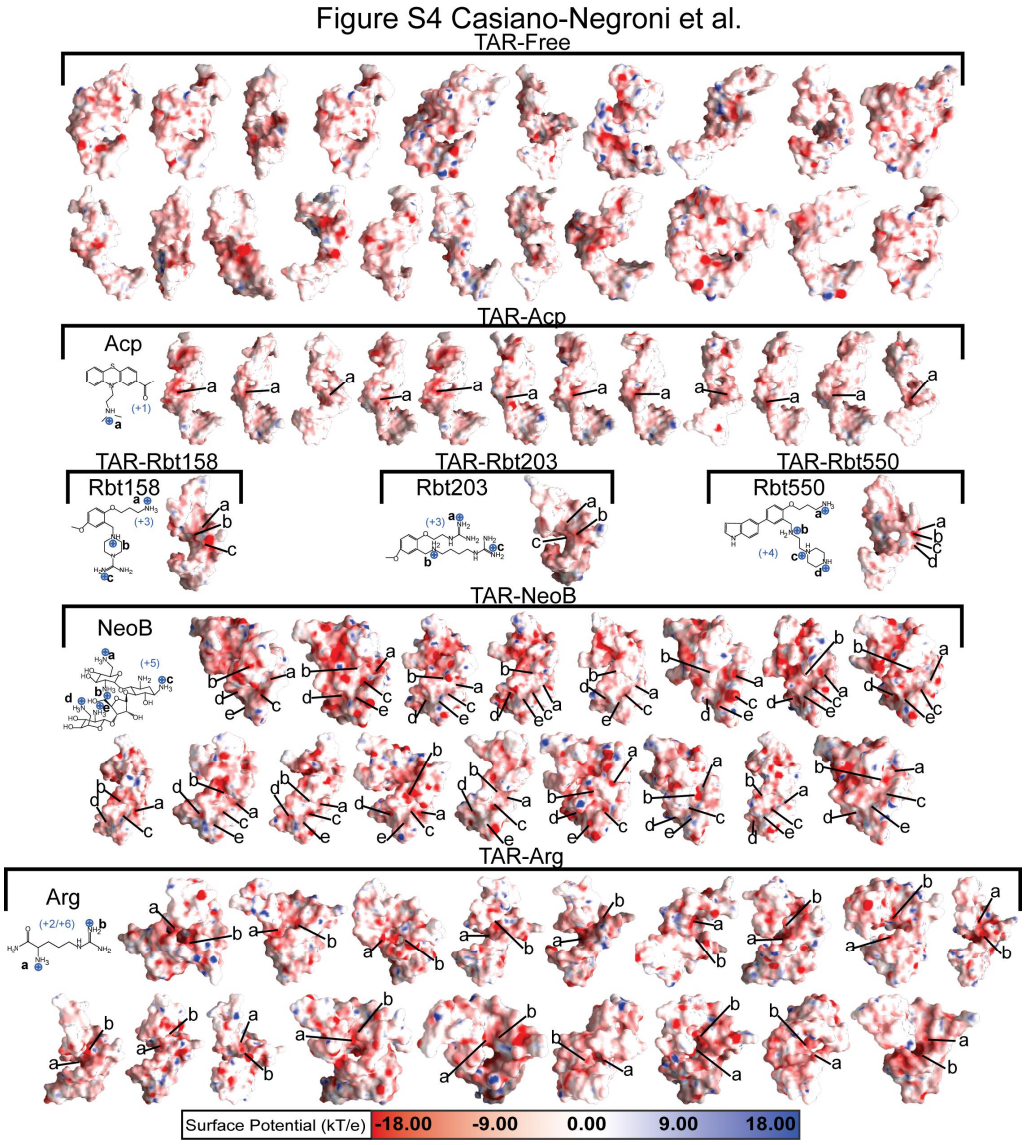

Figure S5. Simulations supporting the validity of Equation 2 for TAR under two-state averaging. Shown are the dynamically averaged ϑ_{int} and θ values as a function of the fractional population ($p_{(bound)}$) of a "bound" state for a two state model involving a "free" TAR conformation with ϑ_{int} = 0.6 and θ = 51 and a "bound" TAR conformation with ϑ_{int} = 1.0 and θ = 0. The dashed line represents the population weighted average values of ϑ_{int} and θ obtained using Equation 2. The circles represent explicit ϑ_{int} and θ values obtained from motional averaging of the free and bound RDCs. The latter were computed as following. An alignment tensor was computed for the TAR conformation at 25 mM Na^+ using the program PALES (*1*). The computed alignment tensor frame was used together with the TAR conformation to predict the "free" RDCs assuming an S_{zz} value of 1.0 x 10^{-3} and η = 0.2. The stem II RDCs were then uniformly scaled down by a factor of 0.6 to simulate ϑ_{int} = 0.6. The "bound" RDCs were computed for a linear TAR conformation using an alignment tensor frame computed using PALES and S_{zz} value of 1.0 x 10^{-3} and η = 0.2. No scaling was preformed to simulate ϑ_{int} = 1.0. Population weighted average RDCs ($p_{(bound)}RDC_{(bound} + (1-p_{(bound)})RDC_{(free)}$) were then computed as a function of $p_{(bound)}$. The RDCs measured in the two helices were then subjected to an order tensor analysis from which the dynamically averaged values of ϑ_{int} and θ were computed (solid line). Very good agreement is observed between the direct population weighted averaged ϑ_{int} and θ values (dashed line) and those obtained from averaging of the RDCs (solid line).

Figure S5 Casiano-Negroni et al.

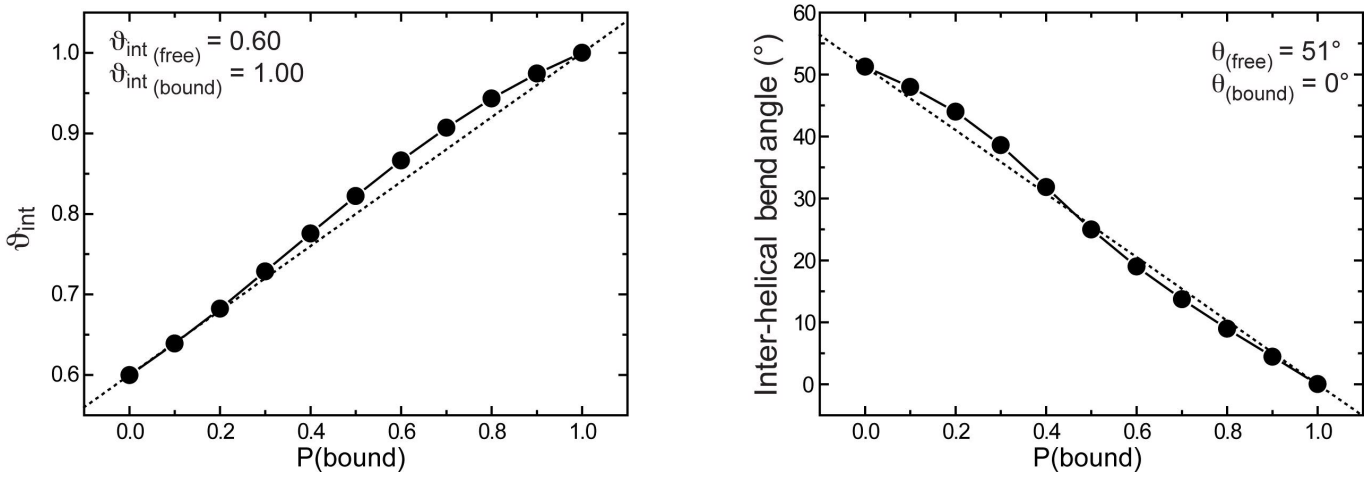

Table S1. One bond CH and NH RDCs (in Hz) measured in TAR under different metal conditions

Residue (bond vector)	160mM NaCl	320mM NaCl	4mM $MgCl_2$
17(C8H8)	-4.5	0.2	0.2
18(C1'H1')	*NA*	-29.5	*NA*
18(C8H8)	0.3	-1.6	-1.8
18(N1H1)	-7.3	*NA*	-2.8
19(C6H6)	9.6	10.0	8.4
20(C1'H1')	-6.6	-19.5	-26.4
20(C8H8)	12.2	16.4	13.6
20(C2H2)	7.9	4.4	6.1
21(C1'H1')	-6.6	-13.0	-19.9
21(C8H8)	15.6	20.8	18.6
21(N1H1)	-6.2	*NA*	-8.5
22(C8H8)	11.7	17.2	16.4
22(C2H2)	4.9	13.6	17.9
40(C1'H1')	-5.7	-8.7	*NA*
40(C5H5)	14.2	14.7	11.6
41(C6H6)	11.8	15.2	12.6
41(C5H5)	11.1	11.2	13.8
42(N3H3)	-5.6	*NA*	-7.8
43(C1'H1')	14.6	7.4	*NA*
43(C8H8)	13.0	15.5	11.9
43(N1H1)	-4.3	*NA*	-2.7
44(C6H6)	1.3	1.2	*NA*
44(C5H5)	12.0	17.2	*NA*
45(C1'H1')	2.9	-1.1	-16.9
45(C6H6)	-5.0	-4.3	-6.9
45(C5H5)	9.9	11.3	*NA*
23(C1'H1')	3.4	3.3	0.6

23(C6H6)	8.4	8.3	5.3
23(C5H5)	-0.5	0.2	0.5
24(C5H5)	1.1	-1.5	-1.7
25(C5H5)	4.7	4.5	2.3
26(C1'H1')	-16.4	-17.8	5.7
26(C8H8)	16.9	17.9	17.3
26(N1H1)	-4.0	*NA*	-8.0
27(C1'H1')	-14.5	-13.6	-12.0
27(C8H8)	14.6	14.8	12.4
27(C2H2)	16.9	13.7	16.3
28(C1'H1')	-8.9	-12.8	-11.5
28(C8H8)	16.5	18.3	14.6
28(N1H1)	*NA*	*NA*	-8.4
29(C6H6)	20.9	22.4	18.1
29(C5H5)	8.3	7.1	12.8
31(C1'H1')	-1.8	-8.4	-8.3
31(C6H6)	18.1	19.9	15.6
31(C5H5)	16.6	19.1	15.0
32(C1'H1')	8.1	13.1	11.7
32(C6H6)	9.4	10.0	10.1
32(C5H5)	6.4	12.4	10.3
33(C1'H1')	-10.5	-12.4	-10.3
33(C6H6)	4.2	6.4	6.8
33(C5H5)	0.6	0.8	0.8
34(C1'H1')	6.6	9.9	9.9
34(C8H8)	10.0	14.9	14.4
34(N1H1)	-5.6	*NA*	-9.3
36(C8H8)	22.9	25.3	22.5
36(N1H1)	-10.1	*NA*	-8.9
37(C5H5)	20.6	22.1	15.4
38(C1’H1’)	*NA*	*NA*	-8.6
38(C6H6)	*NA*	16.8	15.6

38(C5H5)	19.9	25.2	19.9
38(N3H3)	-6.5	*NA*	-6.5
39(C5H5)	19.6	23.6	16.4

REFERENCES.

(1) Zweckstetter, M., and Bax, A. (2000) Prediction of sterically induced alignment in a dilute liquid crystalline phase; aid to protein structure determination by NMR. *J . Am. Chem. Soc. 122*, 3791-3792.